

Buried, Charged, Non-Ion-Paired Aspartic Acid 76 Contributes Favorably to the Conformational Stability of Ribonuclease T₁[†]

Anthony Giletto^{‡,§} and C. Nick Pace^{*,‡}

Departments of Medical Biochemistry & Genetics, Biochemistry & Biophysics, and Center for Macromolecular Design, Texas A & M University, College Station, Texas 77843-1114

Received June 22, 1999; Revised Manuscript Received August 9, 1999

ABSTRACT: The side-chain carboxyl of Asp 76 in ribonuclease T1 (RNase T1) is buried, charged, non-ion-paired, and forms three good intramolecular hydrogen bonds (2.63, 2.69, and 2.89 Å) and a 2.66 Å hydrogen bond to a buried, conserved water molecule. When Asp 76 was replaced by Asn, Ser, and Ala, the conformational stability of the protein decreased by 3.1, 3.2, and 3.7 kcal/mol, respectively. The stability was measured as a function of pH for wild-type RNase T1 and the D76N mutant and showed that the pH dependence below pH 3 was almost entirely due to Asp 76. The pK of Asp 76 is 0.5 in the native state and 3.7 in the denatured state. Thus, the hydrogen bonding of the carboxyl group of Asp 76 contributes more than half of the net stability of RNase T1 at pH 7. In addition, the charged carboxyl of Asp 76 stabilizes structure in the denatured states of RNase T1 that is not present in D76N, D76S, and D76A.

Most charged groups are exposed to solvent on the surface of proteins (1, 2); consequently, there is special interest in charged groups that are buried. Rashin and Honig (3) have shown that, on average, there are two buried ionizable groups per protein and 80% of these are ion paired. We focus here on buried carboxyl groups. Buried carboxyls generally stabilize proteins by forming hydrogen-bonded ion pairs, and several examples have been studied: Asp 194 in chymotrypsin (4); Asp 10 and Asp 70 in T4 lysozyme (5, 6); Glu 58 in RNase T1 (7); Asp 102 and Asp 148 in RNase HI (8); Asp 17 in λ repressor (9); Asp 83 and 93 in barnase (10, 11); Glu 36 in Arc Repressor (12); Asp 83 in xylanase (13), and Asp 121 in ribonuclease A (14). In contrast, buried carboxyls that form charge-neutral hydrogen bonds leave an unpaired charge, and these groups have been studied less (13, 15, 16). Asp 76 in RNase T1 provides an example of a carboxyl that is buried, charged, and not ion paired.

For most proteins, including RNase T1, a bell-shaped dependence of stability on pH is observed with the maximum stability near the isoelectric pH (17). An early explanation for this was that Coulombic repulsion among groups of like charge at high and low pH was greater in the folded than in the unfolded protein leading to decreases in stability at pH extremes. Although Coulombic repulsion is a contributing factor, it also promotes differences in pKs for ionizable groups in the folded and unfolded states of the protein which contribute to the pH dependence of the stability (18). For example, the stability of RNase T1 increases as the pH decreases from 9 to 5, and this is almost entirely due to the

difference in pKs of the histidine side chains in the folded and unfolded states (7). The histidines have higher pKs in the folded state than in the unfolded states so increasing H⁺ concentration shifts the folding equilibrium toward the folded state and the stability increases. Below pH 5, the stability of RNase T1 decreases sharply (19). This reflects increasing Coulombic repulsion among the positive charges, as well as the fact that some of the carboxyl groups have lower pKs in the folded than in the unfolded protein (20–22). The goal of this work was to determine the contribution of the buried carboxyl of Asp 76 to the pH dependence of the stability of RNase T1. We show that Asp 76 makes a large contribution to the stability of RNase T1, and dominates the pH dependence of the stability below pH 5.

EXPERIMENTAL PROCEDURES

Materials. RNase T1 and the mutants were prepared as previously described (23).

Methods. Urea and thermal denaturation curves were determined and analyzed as previously described (23, 24). The buffers (30 mM) used were pH 8 (diglycine), pH 7 (Mops), pH 6.5–5.5 (Mes), pH 5.0 to 3.4 (formic acid), pH 2.7 to 1.8 (glycine). At pH <1.8, no buffer was used. The pH given for each experiment was determined by measuring the pH of samples near the midpoint of the transition region after the experiment with a Radiometer Model 83 pH meter calibrated with two pH standards.

RESULTS

Conformational Stability at pH 7. The conformational stability of RNase T1 and the three mutants of Asp 76 was determined by analyses of urea and thermal denaturation curves. The results at pH 7 are summarized in Table 1. The urea denaturation of RNase T1 and all mutants studied to date is reversible and closely approaches a two-state mech-

[†] This research was supported by the National Institutes of Health (GM37039), the Robert A. Welch Foundation (A-1060), and the Tom and Jean McMullin Professorship.

* To whom correspondence should be addressed. Phone: (409) 845-1788. Fax: (409) 847-9481. E-mail: nickpace@tamu.edu.

[‡] Texas A & M University.

[§] Current address: Lynntech, Inc., 7610 Eastmark Drive, Suite 105, College Station, Texas 77840.

Table 1: Parameters Characterizing the Urea and Thermal Unfolding of RNase T1 and Three Asp 76 Mutants at pH 7^a

Protein	urea denaturation ^b			thermal denaturation ^c		
	<i>m</i> (cal/mol M)	(urea) _{1/2} (M)	Δ(Δ <i>G</i>) (kcal/mol)	Δ <i>H</i> _m (kcal/mol)	<i>T</i> _m (°C)	Δ(Δ <i>G</i>) (kcal/mol)
RNase Sa	1140	6.43		96.6	50.8	
D76N	1410	3.01	3.1	76.0	37.0	3.1
D76S	1360	2.99	3.3	77.6	37.2	3.1
D76A	1420	2.57	3.7	71.1	35.6	3.8

^a The urea and thermal denaturation curves were determined in 30 mM Mops, pH 7. The urea denaturation curves were determined at 15 °C.

^b The values of *m* and (urea)_{1/2} are based on analyses of urea denaturation data using eq 1. (urea)_{1/2} = Δ*G*(H₂O)/*m*. Δ(Δ*G*) = Δ*G*(H₂O)(wild-type) − Δ*G*(H₂O)(mutant). Average values based on three urea denaturation curves are given and the uncertainties are ±40 cal/mol M for *m*, ±0.03 M for (urea)_{1/2}, and ±0.2 kcal/mol for Δ(Δ*G*). ^c The values of Δ*H*_m and *T*_m were used with the Δ*C*_p values from Table 2 in eq 2 to calculate the stability of the proteins at 15 °C, Δ*G*(15 °C). Δ(Δ*G*) = Δ*G*(15 °C) (wild-type) − Δ*G*(15 °C) (mutant). Average values for two curves are given and the uncertainties are ±7 kcal/mol for Δ*H*_m, ±0.3 °C for *T*_m, and ±0.3 kcal/mol for Δ(Δ*G*).

anism (25, 26). The urea denaturation curves were determined at 15 °C to stabilize the mutants and give longer pretransition baselines to improve the accuracy of the results. The data were analyzed by the linear extrapolation method

$$\Delta G = \Delta G(\text{H}_2\text{O}) - m(\text{urea}) \quad (1)$$

where *m* is a measure of the dependence of Δ*G* on urea concentration and Δ*G*(H₂O) is an estimate of the conformational stability of the protein that assumes that the linear dependence of Δ*G* on urea concentration observed in the transition region extends to 0 M urea (27). Note that the *m* values for the mutants are substantially larger than for wild-type RNase T1. The reasons for this will be considered in the Discussion. As a consequence, the Δ(Δ*G*) values were derived by taking the difference between the Δ*G*(H₂O) values, rather than by the more common procedure of taking the difference between the (urea)_{1/2} values and multiplying by the average *m* value which in this case yields higher Δ(Δ*G*) values (24).

The thermal denaturation of RNase T1 and all mutants studied to date is reversible and closely approaches a two-state mechanism (25, 26). This is also true for the mutants studied here. For example, differential scanning calorimetry was used to study the thermal denaturation of the mutants, and the ratio of the van't Hoff to calorimetric enthalpies was near unity for all the mutants (data not shown).

Larger Δ(Δ*G*) values than those given in Table 1 are obtained at higher temperatures. For example, at 37 °C the Δ(Δ*G*) values are 3.6 kcal/mol for D76N, 3.6 kcal/mol for D76S, and 4.0 kcal/mol for D76A. However, good agreement with the results from urea denaturation is obtained when Δ(Δ*G*) values are estimated at 15 °C (Table 1). To calculate the Δ(Δ*G*) values at 15 °C required the use of the Gibbs–Helmholtz equation:

$$\Delta G(T) = \Delta H_m(1 - T/T_m) - \Delta C_p[(T_m - T) + T \ln(T/T_m)] \quad (2)$$

and this required a value for the heat capacity change for folding, Δ*C*_p. For our studies of the pH dependence of folding, the most important mutant was D76N. Consequently, we determined Δ*C*_p for RNase T1 and the D76N mutant using the procedure of Pace and Laurents (28). The results are summarized in Table 2. The Δ*C*_p value for RNase T1 is in good agreement with the value determined previously, Δ*C*_p = 1.65 ± 0.20 (28), and slightly greater than Δ*C*_p for the D76N mutant. This method has been shown to give good

Table 2: Δ*C*_p for the Folding of RNase T1 and the Asp 76 → Asn Mutant^a

temp (°C)	<i>m</i> (cal/mol M)	(urea) _{1/2} (M)	Δ <i>G</i> (H ₂ O) (kcal/mol)	Δ <i>C</i> _p ^b (kcal/mol K)
RNase T1 ^c				
25	1170	5.20	6.09	1.52
20	1175	5.71	6.72	1.63
15	1140	6.43	7.34	1.62
10	1175	6.70	7.87	1.60
5	1180	7.04	8.32	1.57
D76N ^c				
25	1435	1.80	2.58	1.53
20	1480	2.39	3.53	1.34
15	1410	3.01	4.25	1.43
10	1515	3.30	5.00	1.33
5	1530	3.63	5.55	1.34

^a The urea denaturation curves were determined at the temperature shown in 30 mM MOPS, pH 7. The values of *m*, (urea)_{1/2}, and Δ*G*(H₂O) were based on an analysis of these curves using eq 1. (urea)_{1/2} = Δ*G*(H₂O)/*m*. The error is estimated to be ±40 cal/mol M for *m*, ±0.03 M for (urea)_{1/2}, and ±0.3 kcal/mol for Δ*G*(H₂O). ^b The values of Δ*C*_p were calculated using the Δ*G*(H₂O) values in this table, the Δ*H*_m and *T*_m values in Table 1, and eq 2 (28). ^c The average Δ*C*_p for RNase T1 is 1.59 ± 0.04. The average Δ*C*_p for D76N is 1.39 ± 0.09.

agreement with Δ*C*_p values determined using differential scanning calorimetry (29).

pH Dependence of the Stability of RNase T1 and D76N. Urea denaturation curves were determined at 15 °C at pH values ranging 0.6–8.0 for RNase T1 and D76N. Figure 1A shows the pH dependence of Δ*G*(H₂O). It is clear that removing Asp 76 has a dramatic effect on the stability and its pH dependence.

DISCUSSION

RNase T1 Denatured States. The results in Table 1 show that the *m* values for the mutants are ~20% higher than the *m* value for RNase T1. This might reflect the presence of a higher concentration of an intermediate present at equilibrium for the wild-type protein (27). This is unlikely since there is considerable evidence that the folding of RNase T1 closely approaches a two-state mechanism (26, 30). More likely, it reflects the fact that the mutants unfold to a greater extent than the wild-type protein, an explanation promoted by Shortle for the *m*⁺ mutants of staph nuclease (31). If so, it suggests that Asp 76 stabilizes a pocket of structure in the denatured state that is less stable in the mutants. We have previously shown that RNase T1 does not unfold as completely as barnase (32), and there is evidence that barnase

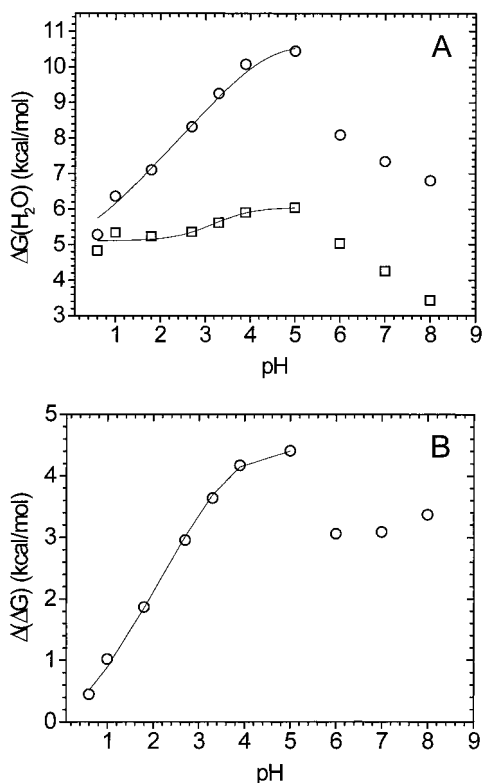


FIGURE 1: (A) $\Delta G(\text{H}_2\text{O})$ at 15 °C vs pH for RNase T1 (circles) and D76N (squares). The solid lines were obtained by fitting the data between pH 0.6 and 5 to eq 4. The fitted parameters obtained for D76N were $pK_{i,N} = 2.8 \pm 0.4$, $pK_{i,D} = 3.5 \pm 0.4$, $\Delta G(\text{H}_2\text{O}) - ([\text{H}^+] = \infty) = 5.1 \pm 0.1$ kcal/mol. If these parameters for D76N are fixed for the analysis of RNase T1, then the fitted parameters obtained are $pK_{i,N} = 0.4 \pm 0.1$ and $pK_{i,D} = 3.7 \pm 0.2$. (B) $\Delta(\Delta G)$ at 15 °C vs pH. The solid line was obtained by fitting the data between pH 0.6 and 5 to eq 5. The fitted parameters obtained were $pK_{i,N} = 0.5 \pm 0.2$, $pK_{i,D} = 3.7 \pm 0.2$, and $\Delta(\Delta G)([\text{H}^+ = \infty]) = 0.0 \pm 0.2$.

does not unfold completely (10). Thus, urea-denatured RNase T1 has some structure that is destabilized in the mutants. If the charge on Asp 76 is required to stabilize the structure in the denatured state, as the difference between the m values for D76N and RNase T1 suggests, then the difference will disappear at low pH below the pK of Asp 76 in the unfolded state. This is what we observe. The m values become identical below pH 4 showing that the negative charge on Asp 76 is required to stabilize the structure in the unfolded state (data not shown). This may also explain why ΔC_p is lower for D76N than RNase T1. Exposing nonpolar surface increases ΔC_p , but exposing polar surface decreases ΔC_p (33). Thus, our observation that ΔC_p is lower for D76N suggests that more polar surface is exposed to solvent when Asn replaces Asp. What sort of structure could be stabilized by the charged carboxyl of Asp 76? One guess is that the side chains of Asp 76 and Arg 77 form a salt bridge in the denatured state when the carboxyl bears a negative charge, but not otherwise. This would also account for the low pK that we observe for Asp 76 in the denatured state, as discussed below. Two turns that are populated in the denatured states of staph nuclease contain -Asp-Lys- and -Asp-Gly-Lys- sequences, so structured regions are not always hydrophobic (34). A seven residue sequence that is partially structured in a denatured SH3 domain is destabilized by GdnHCl (35), but a hydrophobic cluster that is present

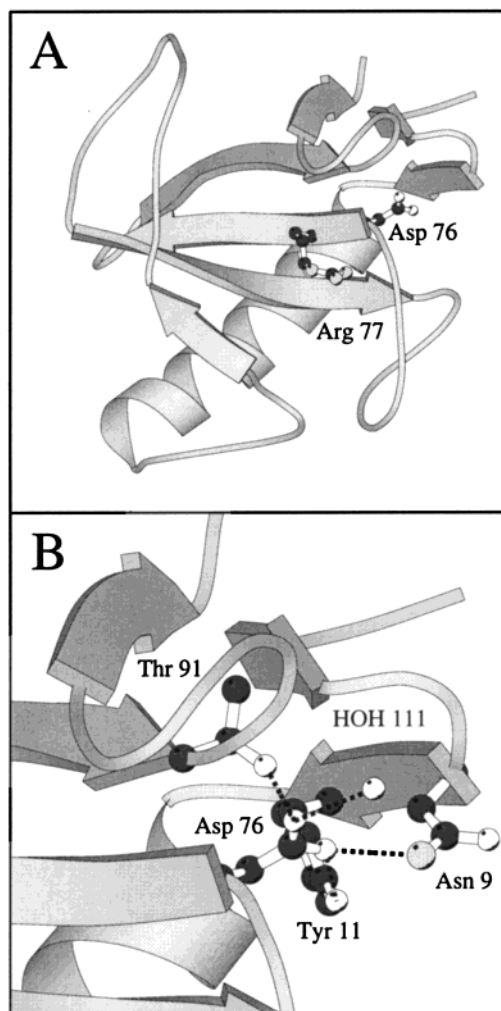


FIGURE 2: (A) Ribbon diagram of RNase T1 showing the side chains of Asp 76 and Arg 77. The charge on the side chain of Arg 77 is the closest positive charge to the negative charge on the side chain of Asp 76, and the distance is at least 6.4 Å so they are not ion paired. (B) A view of the side chain of Asp 76 with the same orientation as in panel A to show the three intramolecular hydrogen bonds (2.63 Å to Thr 91; 2.69 Å to Tyr 11; and 2.89 Å to Asn 9) and the hydrogen bond to water 111 (2.63 Å). The figure was created with MOLSCRIPT (54) based on the 1.5 Å crystal structure (40). The HBPLUS program was used to calculate the hydrogen bond distances (41).

in a urea- or GdnHCl-denatured WW domain is not present in the thermally denatured states (36). Thus, our understanding of the denatured states of proteins is slowly improving, but few general principles have emerged (37).

Contribution of Asp 76 to RNase T1 Stability. As shown in Figure 2, the side chain of Asp 76 is 99% buried (1) and forms hydrogen bonds with a water molecule (2.63 Å) that is conserved in the microbial ribonuclease family (38, 39) and three intramolecular hydrogen bonds: Asp 76 OD1 to OG1 Thr 91 (2.63 Å), Asp 76 OD2 to OH Tyr 11 (2.69 Å), and Asp 76 OD2 to ND2 Asn 9 (2.89 Å) based on the 1.5 Å crystal structure (40), and the HBPLUS program (41). The distance to the two nearest positive charges is 6.4 Å to Arg 77 and 8.5 Å to His 92, and the distance to the N of Ser 13 at the N-terminus of the α -helix is 12.9 Å. When the carboxyl group is removed completely (D76A), the stability decreases by 3.7 kcal/mol. When Ala replaces Asp, a 27 Å³ cavity might be created (42). The cost of cavity formation is 22

cal/Å³ (43), so this could amount to 0.6 kcal/mol favoring wild-type RNase T1. On the other hand, the difference in conformational entropy between the side chains would favor the mutant by about 0.8 kcal/mol (44). Thus, it is clear that the loss in stability must reflect more than just the creation of a cavity or a difference in side-chain conformational entropy. The hydrogen bonding and van der Waals interactions of this charged carboxyl group in the folded protein must be much more favorable than the same interactions with water and/or protein in the unfolded protein. Potentially, the D76A mutant could have four unsatisfied hydrogen bonds that would be highly destabilizing relative to the unfolded state.

For D76S and D76N, the stability decrease is smaller, ~3.1 kcal/mol. For D76S, this indicates that the -OH group has a more favorable interaction in the folded than in the unfolded protein. Modeling shows that Ser 76 could form a ~2.8 Å hydrogen bond with the -OH of Tyr 11, and our results suggest that it does. D76N is more complicated. The Asn side chain is ~10 Å³ larger than an Asp side chain, so some steric strain is possible (42). The carbonyl O of Asn will still be able to hydrogen bond, but now they will be neutral rather than charge-neutral hydrogen bonds. Since the -NH₂ group of the Asn can only serve as a hydrogen bond donor, the hydrogen bonds by one of the oxygens of Asp will be lost. Despite the fact that there is no adjacent positive charge, the site was obviously designed for a carboxyl group and the protein is much less stable when an amide group is substituted.

pH Dependence of RNase T1 Stability. The pH dependence of the stability is shown in Figure 1. These data can be used to estimate the number of protons, *n*, bound or released on unfolding using

$$\Delta[\Delta G(\text{H}_2\text{O})]/\Delta(\text{pH}) = 2.303RTn \quad (3)$$

In the pH range 6–9, RNase T1 and D76N release about the same number of protons on unfolding (~1), and this results because the His residues have higher *pK*s in the folded than in the unfolded protein (7). In the pH range below 5, RNase T1 and D76N bind protons on unfolding, but RNase T1 binds ~1 more proton than D76N. This is clear from Figure 1A where the pH dependence of $\Delta G(\text{H}_2\text{O})$ is much greater for RNase T1 than D76N. (We previously estimated that a maximum of ~1.7 protons are bound by RNase T1 on unfolding (19).) Since the pH dependence of the stability above pH 5 was considered previously (7), here we focus our attention on the pH dependence below pH 5.

Tanford (18) showed that the pH dependence of the stability of a protein can be described by the following equation:

$$\Delta G(\text{H}_2\text{O}) = \Delta G(\text{H}_2\text{O})([\text{H}^+] = 8) + RT \ln \sum_i ([1 + K_{i,N}/[\text{H}^+]]/[1 + K_{i,D}/[\text{H}^+]]) \quad (4)$$

where $\Delta G(\text{H}_2\text{O})([\text{H}^+] = \infty)$ is $\Delta G(\text{H}_2\text{O})$ for the fully protonated protein, $K_{i,D}$ and $K_{i,N}$ are the dissociation constants of group *i* in the denatured and native conformations, respectively, and $[\text{H}^+]$ is the hydrogen ion activity. Previously, we were able to account for the pH dependence of the stability from pH 5 to 2 without assigning any group a $pK_{i,N}$ less than 2.7 (19). In this study, we have extended the

measurements to pH 0.6, and it is clear that a group with a $pK_{i,N}$ below 2.7 is needed to account for the observed pH dependence. We fit the pH data between pH 0.6 and 5 for D76N to eq 4 and found $pK_{i,N} = 2.8 \pm 0.4$, $pK_{i,D} = 3.5 \pm 0.4$, and $\Delta G(\text{H}_2\text{O})([\text{H}^+] = \infty) = 5.1 \pm 0.1$ kcal/mol (Figure 1A). (Most likely, these *pK*s do not correspond to a single group, but are average values for more than one group.) Assuming that the contribution is the same in RNase T1, we find that another group with $pK_{i,N} = 0.4 \pm 0.1$ and $pK_{i,D} = 3.7 \pm 0.3$ is required to fit the data (Figure 1A).

Several groups have used analyses of plots of $\Delta(\Delta G)$ vs pH to obtain an estimate of the $pK_{i,N}$ and $pK_{i,D}$ values for the ionizable group that differs between the wild-type and mutant proteins (14, 20, 21, 45–47). The data in Figure 1A were used to generate such a plot for RNase T1 and D76N (Figure 1B). It is obvious that a difference in *pK* for a single ionizable group cannot describe the data over the pH range studied. As the pH decreases from 7 to 4, the net charge on RNase T1 increases from -8 to 0, and below 4 it will then increase from 0 to +7. Thus, Asp76 will experience an increasingly favorable Coulombic interaction with the rest of the charges in RNase T1 as the pH decreases below 7, but this will not occur in D76N. This factor would cause the $\Delta(\Delta G)$ value to increase as the pH decreases, and is probably why the stability increases as the pH decreases from 8 to 5. (This assumes that the contribution of His ionization will be the same in RNase T1 and D76N.) However, as the pH decreases below 5, the *pK* difference for Asp 76 in the native and denatured states will dominate and cause $\Delta(\Delta G)$ to decrease. If we fit the data below pH 5 to this equation (14),

$$\Delta(\Delta G) = \Delta(\Delta G)([\text{H}^+] = \infty) + RT \ln([1 + K_{i,N}/[\text{H}^+]]/[1 + K_{i,D}/[\text{H}^+]]) \quad (5)$$

we find $pK_{i,N} = 0.5 \pm 0.2$, $pK_{i,D} = 3.7 \pm 0.1$, and $\Delta(\Delta G)([\text{H}^+] = \infty) = 0.0 \pm 0.2$ (Figure 1B). On the basis of these analyses, we estimate that the *pK* of Asp 76 is 0.5 ± 0.1 in native and 3.7 ± 0.2 in denatured RNase T1.

pKs of Asp Carboxyls in Native and Denatured Proteins. In an unstructured peptide in the absence of other charged groups, a $pK_{\text{int}} = 4.1 \pm 0.1$ is expected for the carboxyl group of an Asp side chain, and a distinctly higher $pK_{\text{int}} = 4.5 \pm 0.1$ is expected for the carboxyl group of a Glu side chain (48). [Recently, Kuhlman et al. (22) have shown that these *pK* values are sequence dependent in short peptides.] Thus, the $pK_D = 3.7$ that we observe for Asp 76 indicates that some feature of the denatured state of RNase T1 is lowering the *pK*. A more nonpolar environment would be expected to raise the *pK* as would Coulombic interactions with negative charges. In contrast, Coulombic interactions with positive charges would be expected to lower the *pK*, and we think this is the case in denatured RNase T1. The other possibility is formation of a salt bridge with Arg 77 or another positive charge, as discussed above. The pH dependence of the stability of barnase suggested pK_D values of 3.5 for Asp and 3.7 for Glu (10), and similar studies of chymotrypsin inhibitor 2 suggested pK_D values of 3.6 for Asp and 4.0 for Glu (20). The ionic strength dependence of these pK_D values suggested that Coulombic interactions were of primary importance (20). (Both of these proteins are basic,

with more than twice as many positive charges per residue as RNase T1.) Computational studies have also suggested that introducing electrostatic interactions among groups in denatured proteins is important in accounting for experimental studies of the pH dependence of protein stability (49, 50). In summary, the low pK for Asp 76 in denatured RNase T1 probably reflects net favorable Coulombic interactions with the positive charges on the protein and we expect most of the carboxyls in RNase T1 will have pK s less than those expected based on the model compound values noted above.

The $pK_N = 0.5$ that we find for Asp 76 is among the lowest observed for carboxyl groups in proteins. As noted above, carboxyl groups in nonpolar environments are expected to have elevated pK s and many have been observed. For example, for carboxyls in nonpolar environments that were not designed for carboxyl groups, we found $pK_N = 5.7$ for Asp 44 in N44D RNase T1 (23), and Dao-pin et al. (51) found $pK_N \approx 6.2$ for Asp 133 in L133D T4 lysozyme. [See Garcia-Moreno et al. (52) for other examples and a thorough discussion.] In addition, carboxyl groups near negative charges will have elevated pK s. For example, Walter et al. (46) found $pK_N = 5.9$ for Glu 28 in RNase T1, which is at the carboxyl terminus of the α -helix with Asp 29 and Glu 31 nearby.

However, most carboxyls in native proteins have pK s significantly lower than the pK_{int} values noted above. For 19 Asp carboxyls, the average pK was 2.7, and for 12 Glu carboxyls, the average pK was 4.0 (53). We will now focus our attention specifically on the carboxyl groups of Asp side chains. Gandini et al. (2) have analyzed Asp residues in 44 high-resolution, nonhomologous protein structures. They find that 34% of the Asp carboxyls have no intramolecular interactions, 34% form charge-neutral hydrogen bonds, and 32% form salt bridges (28% with charge-charge hydrogen bonds and 4% without hydrogen bonds). Several Asp carboxyls involved in salt bridges have been found to have very low pK_N values: $pK_N < 2$ (Asp 83 in xylanase, the protein must unfold to protonate this Asp) (13); $pK_N \approx 0.7$ (Asp 93 in barnase) (10); $pK_N < 0.5$ (Asp 10 and 70 in T4 lysozyme) (5, 6). Asp carboxyls that form charge-neutral hydrogen bonds in the absence of a salt bridge can also have very low pK_N values as our results with Asp 76 show. (Recall, the nearest positive charge is 6.4 Å away.) Another example is Asp 101 in xylanase, which has a $pK < 2$ and does not protonate until the protein unfolds (13). In considering these low pK_N values, it appears that good hydrogen bonding may be more important than ion pairing or longer range Coulombic interactions in stabilizing these buried carboxylate groups.

Concluding Opinions. It is clear that the charged carboxyl of Asp 76 makes a substantial contribution to the conformational stability of RNase T1 when it is buried in the interior of the protein with a $pK_N = 0.5$. This remarkably low pK depends more on the formation of four excellent hydrogen bonds than on a net favorable Coulombic interaction with other charged groups. It is also clear that a buried carboxyl that is not hydrogen bonded would have a $pK_N > 6$ (52). When the RNase T1 is denatured, the charged carboxyl of Asp 76 stabilizes some structural element and has a $pK_D = 3.7$. It is clear that the pK_D value is lower than expected because of net favorable Coulombic interac-

tions with the other charged groups (20). It is not clear what the structure in the denatured state might be or how it is stabilized. These are important questions that we hope to answer.

ACKNOWLEDGMENT

We thank Andy Robertson, Jerry Grimsley, Kevin Shaw, Bea Huyghues-Despointes, and Marty Scholtz for helpful discussions and Kevin Shaw for preparing Figure 2.

REFERENCES

- Lee, B., and Richards, F. M. (1971) *J. Mol. Biol.* 55, 379–400.
- Gandini, D., Gogioso, L., Bolognesi, M., and Bordo, D. (1996) *Proteins* 24, 439–449.
- Rashin, A. A., and Honig, B. (1984) *J. Mol. Biol.* 173, 515–521.
- Fersht, A. R. (1972) *J. Mol. Biol.* 64, 497–509.
- Anderson, D. E., Becktel, W. J., and Dahlquist, F. W. (1990) *Biochemistry* 29, 2403–2408.
- Anderson, D. E., Lu, J., McIntosh, L., and Dahlquist, F. W. (1993) in *NMR of Proteins* (Clore, G. M., and Gronenborn, A. M., Eds.) Macmillan.
- McNutt, M., Mullins, L. S., Raushel, F. M., and Pace, C. N. (1990) *Biochemistry* 29, 7572–7576.
- Oda, Y., Yamazaki, T., Nagayama, K., Kanaya, S., Kuroda, Y., and Nakamura, H. (1994) *Biochemistry* 33, 5275–5284.
- Marqusee, S., and Sauer, R. T. (1994) *Protein Sci.* 3, 2217–2225.
- Oliveberg, M., Arcus, V. L., and Fersht, A. R. (1995) *Biochemistry* 34, 9424–9433.
- Tissot, A. C., Vuilleumier, S., and Fersht, A. R. (1996) *Biochemistry* 35, 6786–6794.
- Waldburger, C. D., Schilldbach, J. F., and Sauer, R. T. (1995) *Struct. Biol.* 2, 122–128.
- Joshi, M. D., Hedberg, A., and McIntosh, L. P. (1997) *Protein Sci.* 6, 2667–2670.
- Quirk, D. J., Park, C., Thompson, J. E., and Raines, R. T. (1998) *Biochemistry* 37, 17958–17964.
- Peterson, R. W., Nicholson, E. M., Thapar, R., Klevit, R. E., and Scholtz, J. M. (1999) *J. Mol. Biol.* 286, 1609–1619.
- Schaller, W., and Robertson, A. D. (1995) *Biochemistry* 34, 4714–4723.
- Pace, C. N. (1990) *Trends Biochem. Sci.* 15, 14–17.
- Tanford, C. (1970) *Adv. Protein Chem.* 24, 1–95.
- Pace, C. N., Laurents, D. V., and Thomson, J. A. (1990) *Biochemistry* 29, 2564–2572.
- Tan, Y. J., Oliveberg, M., Davis, B., and Fersht, A. R. (1995) *J. Mol. Biol.* 254, 980–992.
- Swint-Kruse, L., and Robertson, A. D. (1995) *Biochemistry* 34, 4724–4732.
- Kuhlman, B., Luisi, D. L., Young, P., and Raleigh, D. P. (1999) *Biochemistry* 38, 4896–4903.
- Hebert, E. J., Giletto, A., Sevcik, J., Urbanikova, L., Wilson, K. S., Dauter, Z., and Pace, C. N. (1998) *Biochemistry* 37, 16192–16200.
- Pace, C. N., Scholtz, J. M. (1997) in *Protein Structure: a practical approach* (Creighton, T. E., Ed.) pp 299–321, IRL Press, Oxford.
- Shirley, B. A., Stanssens, P., Hahn, U., and Pace, C. N. (1992) *Biochemistry* 31, 725–732.
- Thomson, J. A., Shirley, B. A., Grimsley, G. R., and Pace, C. N. (1989) *J. Biol. Chem.* 264, 11614–11620.
- Pace, C. N. (1986) *Methods Enzymol.* 131, 266–280.
- Pace, C. N., and Laurents, D. V. (1989) *Biochemistry* 28, 2520–2525.
- Pace, C. N., Grimsley, G. R., Thomas, S. T., and Makhatadze, G. I. (1999) *Protein Sci.* 8, 1500–1504.
- Yu, Y., Makhatadze, G. I., Pace, C. N., and Privalov, P. L. (1994) *Biochemistry* 33, 3312–3319.
- Shortle, D. (1995) *Adv. Protein Chem.* 46, 217–247.

32. Pace, C. N., Laurents, D. V., and Erickson, R. E. (1992) *Biochemistry* 31, 2728–2734.
33. Makhataadze, G. I., Lopez, M. M., and Privalov, P. L. (1997) *Biophys. Chem.* 64, 93–101.
34. Wang, Y., and Shortle, D. (1997) *Folding Des.* 2, 93–100.
35. Zhang, O., and Forman-Kay, J. D. (1997) *Biochemistry* 36, 3959–3970.
36. Koepf, E. K., Petrassi, H. M., Sudol, M., and Kelly, J. W. (1999) *Protein Sci.* 8, 841–853.
37. Smith, L. J., Fiebig, K. M., Schwalbe, H., Dobson, C. M. (1996) *Folding Des.* 1, R95–R106.
38. Langhorst, U., Loris, R., Denisov, V. P., Doumen, J., Roose, P., Maes, D., Halle, B., and Steyaert, J. (1999) *Protein Sci.* 8, 722–730.
39. Malin, R., Zielenkiewicz, P., and Saenger, W. (1991) *J. Biol. Chem.* 266, 4848–4852.
40. Martinez-Oyanedel, J., Choe, H.-W., Heinemann, U., and Saenger, W. (1991) *J. Mol. Biol.* 222, 335–352.
41. McDonald, I. K., and Thornton, J. M. (1994) *J. Mol. Biol.* 238, 777–793.
42. Harpaz, Y., Gerstein, M., and Chothia, C. (1994) *Structure* 2, 641–649.
43. Xu, J., Baase, W. A., Baldwin, E., Matthews, B. W. (1998) *Protein Sci.* 7, 158–177.
44. Doig, A. J., and Sternberg, M. J. E. (1995) *Protein Sci.* 4, 2247–2251.
45. Myers, J. K., Smith, J. S., Pace, C. N., and Scholtz, J. M. (1996) *J. Mol. Biol.* 263, 390–395.
46. Walter, S., Hubner, B., Hahn, U., and Schmid, F. X. (1995) *J. Mol. Biol.* 252, 133–143.
47. Stites, W. E., Gittis, A. G., Lattman, E. E., and Shortle, D. (1991) *J. Mol. Biol.* 221, 7–14.
48. Nozaki, Y., and Tanford, C. (1967) *J. Biol. Chem.* 242, 4731–4735.
49. Warwicker, J. (1999) *Protein Sci.* 8, 418–425.
50. Schaefer, M., van Vlijmen, H. W., and Karplus, M. (1998) *Adv. Protein Chem.* 51, 1–57.
51. Dao-Pin, S., Anderson, D. E., Baase, W. A., Dahlquist, F. W., and Matthews, B. W. (1991) *Biochemistry* 30, 11521–11529.
52. Garcia-Moreno, B., Dwyer, J. J., Gittis, A. G., Lattman, E. E., Spencer, D. S., and Stites, W. E. (1997) *Biophys. Chem.* 64, 211–224.
53. Antosiewicz, J., McCammon, J. A., and Gilson, M. K. (1996) *Biochemistry* 35, 7819–7833.
54. Kraulis, P. J. (1991) *J. Appl. Crystallogr.* 24, 946–950.

BI991422S